Pax3 regulates morphogenetic cell behavior in vitro coincident with activation of a PCP/non-canonical Wnt-signaling cascade

O'Neil Wiggan and Paul A. Hamel*

Department of Laboratory Medicine and Pathobiology, University of Toronto, Toronto, Ontario, M5S 1A8 Canada
*Author for correspondence (e-mail: paul.hamel@utoronto.ca)

Accepted 26 October 2001
Journal of Cell Science 115, 531-541 (2002) © The Company of Biologists Ltd

Summary

Mutations to *Pax3* and other Pax family genes in both mice and humans result in numerous tissue-specific morphological defects. Little is known, however, about the cellular and molecular mechanisms by which Pax genes regulate morphogenesis. We previously showed that Pax3 induces cell aggregation and a mesenchymal-to-epithelial transition in Saos-2 cells. We show here that Pax3-induced aggregates arise through the formation of distinct structures involving cell rearrangements and cell behaviors resembling those that occur during gastrulation and neurulation known as convergent extension. During these Pax3-induced processes, Dishevelled and Frizzled are localized to the actin cytoskeleton and both proteins co-immunoprecipitate focal adhesion components from detergent-insoluble cell fractions. We show further that these Pax3-induced cell movements are associated with activation of a Wnt-signaling cascade, resulting in induction and activation of c-Jun-N-terminal kinase/stress activated protein kinase (JNK/SAPK). All of these Wnt-signaling factors exhibit altered subcellular distribution in Pax3-expressing cells. In particular, we show the localization of JNK/SAPK to both the nucleus and to cytoplasmic multi-vesicular structures. These data show that Pax3 regulates morphogenetic cell behavior and that regulation of a conserved, planar cell polarity/non-canonical Wnt-signaling cascade entailing JNK activation is a function of Pax3 activity.

Key words: Pax3, Wnt-signaling, Dishevelled, Focal adhesion, JNK, Frizzled

Introduction

Pax3, a member of the paired-family of transcription factors, is required for a number of fundamental processes during vertebrate development (Dahl et al., 1997). In mice, mutations to Pax3 result in the splotch (*sp*) phenotype which is characterized by a number of early developmental defects (Epstein et al., 1991). These defects, among others, include impaired neural tube closure, absence of limb musculature and the impaired development of several structures derived from the neural crest. In humans, mutations to *Pax3* give rise to the pigmentation, hearing and facio-skeletal anomalies observed in Waardenburg syndrome (Baldwin et al., 1992; Tassabehji et al., 1992). The mechanisms by which *Pax3* and other Pax genes regulate morphological development are poorly understood, however, as the cellular and molecular processes that these genes regulate remain ill defined.

Tissue morphogenesis is characterized by the coordinated effect of several different cell behaviors including changes to cell shape, position, adhesion, proliferation and death (Atchley and Hall, 1991; Gumbiner, 1996). Patterning of the vertebrate neural tube, for example, involves a coordinated set of cell behaviors known as convergent extension, which results in the simultaneous narrowing of the tissue in one dimension and its lengthening in a perpendicular dimension (Colas and Schoenwolf, 2001). Characterization of *Drosophila* and vertebrate morphogenetic mutants has revealed the common use of conserved signaling cascades such as the c-Jun-N-terminal kinase/stress activated protein kinase (JNK/SAPK) pathway during morphogenesis (Noselli, 1998; Noselli and Agnes, 1999; Sokol, 2000). JNK signaling pathways have been specifically implicated in processes such as dorsal closure, thorax closure and in planar tissue/cell polarity (Martin-Blanco et al., 2000; Noselli, 1998; Zeitlinger and Bohmann, 1999). Additionally, a signaling cascade involving a Wnt receptor, Frizzled, and a downstream effector, Dishevelled, is implicated in the regulation of morphogenesis in *Drosophila* and is also coupled to JNK activation in tissue polarization (Sokol, 2000). This Frizzled-mediated signaling cascade, which regulates planar cell polarity (PCP) in *Drosophila*, appears homologous to a Wnt-signaling cascade recently shown to regulate convergent extension movements in vertebrates (Heisenberg et al., 2000; Wallingford et al., 2000).

Numerous studies have suggested a role for Pax genes in the regulation of Wnt signaling (Dahl et al., 1997; Uusitalo et al., 1999). One such study has revealed that the combined activity of Pax3 and Pax7 is required for normal Wnt4 expression in the neural tube during murine development (Mansouri and Gruss, 1998). Analogous to the consequences of mutant Pax genes, mutations to *Wnt* and to *JNK* genes in mice also result in morphological defects in specific tissues. For example, as for *Pax3* mutant mice, mutations to distinct Wnt genes result in neural tube patterning defects (Uusitalo et al., 1999). Thus, on the basis of these and other data, we hypothesized that Pax proteins regulate one or more of the aforementioned

cell behaviors through modulation of signaling cascades controlling morphogenetic cell behavior.

Using an in vitro approach, we recently showed that ectopic Pax3 expression induces cell aggregation and a phenotypic mesenchymal-to-epithelial transition in vitro (Wiggan et al., 2002). This study also confirmed c-met as a direct transcriptional target of Pax3 and showed the ability of Pax3-induced cell aggregates to dissociate in response to hepatocyte growth factor/scatter factor (HGF/SF). In the present study we examined the cellular mechanisms by which Pax3 induced cell aggregation of Saos-2 cells. We show that ectopic Pax3 expression in Saos-2 cells induced cell behaviors that resulted in morphogenetic cell movements similar to those used by cells during vertebrate gastrulation and neurulation. These Pax3-induced morphogenetic cell movements are associated with the induction of a signaling cascade resulting in activation of JNK and in altered subcellular localization of Dishevelled, Frizzled and activated JNK. Our results showing the localization of Dishevelled and Frizzled to the actin cytoskeleton and their redistribution in response to Pax3 expression indicate a novel mechanism by which Pax3 may regulate pattern formation during development.

Materials and Methods

Adenoviruses, plasmids and antibodies

Adtrack adenoviruses expressing $Pax3^{flag}$ or βgal were generated as previously described (Wiggan et al., 2002). Plasmids encoding mutant HA-tagged GSK3 and HA-tagged JNK1 were gifts of J. Woodgett (OCI, Toronto). Anti-JNK antibodies were also a gift of J. Woodgett. Anti-phospho-JNK was obtained from New England Biolabs (NEB). Anti-actin, monoclonal anti-vinculin and FITC-conjugated phalloidin were obtained from Sigma Chemicals (Oakville, ON, Canada). Monoclonal anti-paxillin was obtained from Transduction Laboratories (Lexington, KY). Goat anti-Dishevelled (C-19) and anti-Frizzled (C-17) antibodies were obtained from Santa Cruz Biotechnology (Santa Cruz, CA). FITC- and Texas Red-conjugated secondary antibodies were obtained from Jackson Immuno Research Laboratories (West Grove, PA).

Cell culture

Saos-2 osteosarcoma cells were grown in DMEM supplemented with 10% fetal calf serum (Sigma, Oakville, ON, Canada). For infections, typically 1×10^5 cells were plated on 35 mm plates (Nunc) the day before infection. The following day, cells were infected at a multiplicity of infection (m.o.i.) of 10 in a total of 2 ml of normal media. Additionally, for time-lapse analyses, cultures were overlaid with liquid paraffin. Transfections were done using standard calcium phosphate procedures.

Immunofluorescence staining and microscopy

For methanol/acetone fixation, cells grown on glass coverslips were fixed for 10 minutes in 50% methanol/50% acetone at room temperature. Coverslips were rinsed in PBS and cells were then exposed to a blocking solution of 3% bovine serum albumin (BSA) in PBS for 30 minutes. This fixation procedure efficiently extracted all the green fluorescent protein (GFP), which is co-expressed in both $Ad\text{-}Pax3^{flag}$ and Ad-β-gal adenoviruses, thus enabling dual staining of cells. GFP signals after methanol/acetone fixation were equivalent to those obtained for control staining with FITC-conjugated secondary antibodies alone. For paraformaldehyde fixation cells were fixed in freshly prepared 4% paraformaldehyde for 10 minutes at room temperature followed by exposure to a solution of 0.2% Triton X-100 and 3% bovine serum albumin (BSA) in PBS for 30 minutes for permeabilization and to block nonspecific binding. For paraformaldehyde-cytoskeletal fixation, cells were fixed in 4% paraformaldehyde in the presence of 0.2% Triton X-100 for 10 minutes at room temperature. This fixation procedure was suitable for dual labeling of cytoskeletal components as it resulted in efficient extraction of all cytoplasmic GFP but maintained variable levels of nuclear GFP. After fixation, cells were incubated for 60 minutes at room temperature with the appropriate primary antibodies, diluted in 3% BSA in PBS. Cells were then rinsed briefly 4-5 times with PBS and subsequently incubated sequentially with the appropriate Texas Red- or FITC-conjugated secondary antibodies in 3% BSA in PBS for 50 minutes. After four washes with PBS, coverslips were then mounted with vinol mountant. Fluorescent images were captured either on a Zeiss axiophot microscope equipped with a CCD camera or on a Zeiss LSM confocal microscope. Phase-contrast images were obtained with a Nikon inverted microscope onto Kodak Plus-X pan 125ASA film. Images were processed using Adobe Photoshop software.

Time-lapse videomicroscopy, cell-tracking analysis, protrusion analysis

Time-lapse analyses were carried out in a chamber kept at 37°C and 5% CO_2. Time-lapse recordings were made at 1/240 of real time to a Panasonic time-lapse video recorder with a Hitachi CCD camera connected to an Olympus phase-contrast microscope. Images were captured with either a 10× or 20× objective. Videos were digitized and processed using a Matrox frame grabber and Adobe Premier 5.0 video-processing software. Cell tracings and tracking of centroid positions were carried out using NIH Image software. Analyses of cell protrusive behavior was carried out with NIH image software as described (Elul et al., 1997); 4-10 cells per treatment were analyzed. Cell speed was computed by tracking nuclear positions of at least 25 cells per treatment from two to three videos at 10 or 30 minute intervals, over a 10 hour period using Image-1 software.

Western immunoblots, immunoprecipitation, cell fractionation

Cell fractionation and western blotting were carried out as previously described (Wiggan et al., 2002). Immunoprecipitations were performed by incubating 200 μg of soluble or 100 μg of insoluble extracts with the indicated primary antibodies and protein G-Sepharose beads (Pharmacia) for 2 hours at 4°C. Following this incubation beads were washed five times with lysis buffer, followed by SDS-PAGE and western blotting. The antibodies used for immunoprecipitations and western blotting were the same as those used for cell staining. Quantification of bands was done with NIH image software.

Results

Ectopic Pax3 expression induces morphogenetic cell movements

We recently described the formation in osteogenic Saos-2 cells of Pax3-induced cell aggregates with epithelial characteristics (Wiggan et al., 2002). To better understand the cellular basis of Pax3-induced cell aggregation, a detailed analysis of the cellular processes contributing to the aggregation process was undertaken. As Fig. 1 illustrates, Pax3-induced Saos-2 cell aggregation was a result of distinct cell rearrangements and aggregates formed distinct intermediate structures. At 48 hours postinfection, Ad-β-gal-infected cells were randomly arranged (Fig. 1A). By contrast, up to 40% of $Ad\text{-}Pax3^{flag}$-infected cells

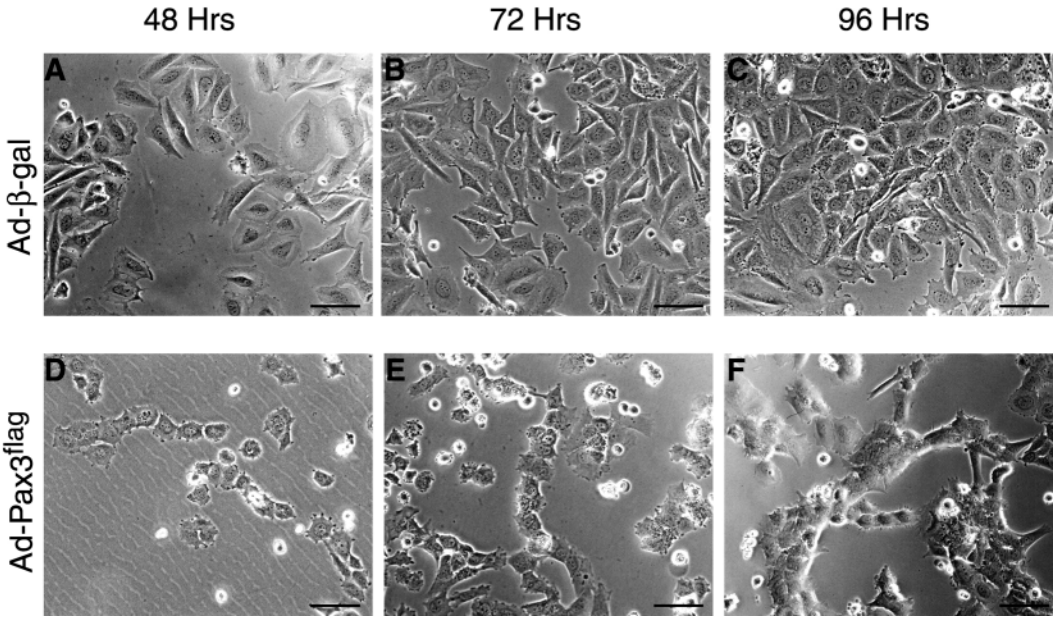

Fig. 1. Formation of distinct cell arrangements during Pax3-induced aggregation of Saos-2 cells. Representative phase-contrast images depicting the arrangement of Saos-2 cells postinfection at the times indicated, infected with control Ad-β-gal infected (A-C) or Ad-Pax3^{flag} (D-E) adenoviruses. Beginning at 48 hours postinfection, in contrast to the random arrangement of control infected cells (A-C), many Pax3-infected cells could be found in columnar (oriented parallel to the plane of the substratum) arrangements (D). These columnar arrangements persisted in Pax3-infected cells as they formed aggregates (E-F). Bars, 80 μm.

could be found arranged in columns, oriented parallel to the plane of the substratum, consisting of three or more cells (Fig. 1D). By 72 hours postinfection, the majority of Ad-Pax3^{flag}-infected cells formed multi-layered aggregates (Fig. 1E). Interestingly, these aggregates maintained columnar arrangements, whereas control infected cells grew to a confluent monolayer (Fig. 1C).

To gain more insight into the cellular basis of these distinct Pax3-induced cell rearrangements, time-lapse video microscopy analyses of Ad-β-gal- or Ad-Pax3^{flag}-infected cultures was performed. Analyses of these recordings revealed a number of distinct cell behaviors contributing to Pax3-induced cell aggregation and rearrangements. For example, between 36 and 72 hours postinfection, Ad-β-gal-infected cells began to exhibit contact inhibition of cell movement (Fig. 2A). By contrast, Ad-Pax3^{flag}-infected cells appeared more motile and displayed both directed and random cell movements (Fig. 2B). Analysis of cell speed indicated the Ad-Pax3^{flag}-infected cells had an average speed of 7.86±2.7 μm/hour, which was 2.5-times greater (P<0.0001) than that of control infected cells (3.05±1.1 μm/hour). In Ad-Pax3^{flag}-infected cells, cell movement was not restricted to individual cells, as cells comprising aggregates also moved cohesively as a group (data not shown).

Pax3^{flag} also induced cell behavior where columns of aggregated cells formed from initially loosely associated and apparently randomly arranged cells. Fig. 3 illustrates the dynamic changes to cell size and shape. Specifically, cells were observed to episodically lengthen and contract over time (compare outline of cells numbered 2 and 3 in Fig. 3A and B). Cell tracings from images captured at selected intervals beginning at 30 hours postinfection revealed that cells underwent rearrangement mediated by both cell migration and cell intercalation. For example, in the 10 hour interval depicted in Fig. 3, cells labeled 2 and 3 in Fig. 3A had migrated upwards to and intercalated between cells 1 and 5 (Fig. 3B). By 83 hours postinfection, through a combination of further reduction in cell size as well as changes in cell shape, increased cell-cell adhesion and cell intercalation, the initially loosely and randomly positioned cells became rearranged into two parallel columns of closely associated cells (data not shown). Taken together, these analyses revealed that cell migration, cell intercalation and alterations to cell shape, cell size and intercellular adhesion properties contributed to the Pax3-induced cell aggregation. These cell behaviors described for the formation of the aggregate illustrated in Fig. 3 contributed to the formation of all Pax3-induced aggregates.

Pax3-induced cell rearrangements beginning around 48 hours postinfection was associated with an increased presence of lamellipodia, filopodia and microspike-like protrusions

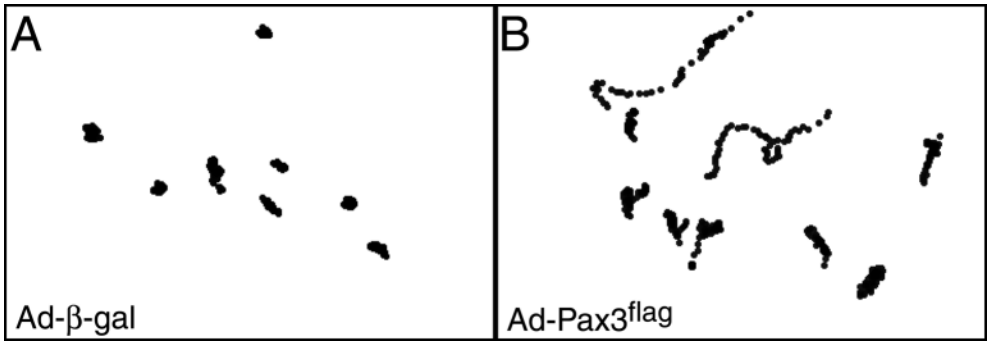

Fig. 2. Ectopic Pax3 expression induces increased cell motility in Saos-2 cells. Paths of individual cells from representative time-lapse recordings are depicted by dots showing centroid positions. Centroid positions were computed at 10 minute intervals over a 10 hour period, at 36 hour postinfection of control infected (A), or Ad-Pax3^{flag}-infected (B) cells.

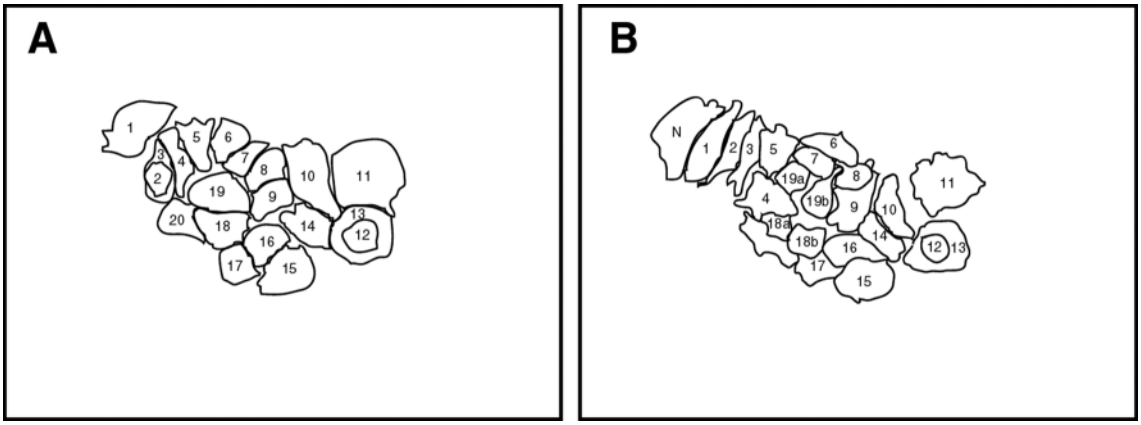

Fig. 3. Sequential time-lapse images depicting cell behaviors underlying the formation of a Pax3-induced columnar cell arrangement. Tracings of cells from selected intervals (A,B) revealed that cell rearrangement occurred by means of cell migration and cell intercalation. (B) Tracing of cells in A 10 hours later. Products of cell division are indicated by the letters a and b. The cell labelled N indicates a new cell that migrated into the field.

(Fig. 4) (Wiggan et al., 2002). Analyses of time-lapse recordings revealed, however, that at 24 hours postinfection, control infected and Pax3-infected cells extended protrusions episodically at similar rates. For protrusions greater than 5 μm in length, control cells extended an average of 8±5 protrusions per cell per hour, whereas an average of 11±3 protrusions per cell per hour in Pax3-infected cells was observed. At this time point for both control and Pax3-infected cells, these protrusions were unstable; up to 60% of protrusions were withdrawn within 5 minutes of extension and 100% of all protrusions withdrew within 25 minutes of extension. Between 36 and 48 hours postinfection there was a significant reduction in the number of protrusions extended by control cells that were greater than 5 μm in length (average of 1±1 protrusion per cell per hour). These cells, however, extended and withdrew many smaller unstable protrusions. By contrast, as cells formed aggregates at 48 hours post-Ad-Pax3^{flag} infection, cells in aggregates extended an average of 4±1 (P=0.001) protrusions per cell per hour. More significantly, these protrusions were considerably more stable than those of control infected cells, with 54% of protrusions in aggregating Pax3-expressing cells persisting for periods up to or greater than 50 minutes. This is in contrast to control infected cells, where there were no protrusions that persisted for 50 minutes or greater. Thus, Pax3-induced cell aggregation is associated with the extension of larger and more persistent protrusions relative to control cells.

The appearance of these persistent protrusions in Pax3-expressing cells was also evident by examining the arrangement of actin in Ad-β-gal vs. Ad-Pax3^{flag}-infected cells (Fig. 4A). As illustrated, at three days postinfection, multiple large actin-containing protrusions in control cells were infrequent, whereas multiple large protrusions were evident in condensed cells expressing Pax3. The episodic nature of these protrusions in Pax3-expressing cells is illustrated in Fig. 4D-F. Persistent protrusions in Pax3-expressing cells, some of which extended over 100 μm in length, were often very elaborate and resembled growth cones (Fig. 4B). Furthermore, during the aggregation process, persistent filopodia-like protrusions from individual cells appeared to 'seek out' and to be directed to neighboring cells, often over extended distances (Fig. 4C, for example). These persistent protrusions were involved in behavior not observed in control cells. Specifically, at 72 to 96 hours postinfection, extension of a filopodia-like protrusion from one aggregate to another typically preceded the frequently observed fusion of neighboring aggregates. So, for example, Fig. 4D-J illustrates the type of cell behavior involved in the fusion of neighboring aggregates and in the recruitment of free cells into aggregates. Following the extension of a filopodia-like protrusion from one cell to another (Fig. 4E), the cell making the protrusion was often observed to extend to the newly contacted cell, creating a bridge between aggregates or to a neighboring cell (Fig. 4F,H-I). Furthermore, cell division, cell migration and cell intercalation appeared to be coordinated during aggregation such that bridges and the columnar arrangement of aggregates were maintained (Fig. 4G,J).

Together, all of the aforementioned cell behaviors culminated in the formation of highly extended three-dimensional structures four to seven days following Ad-Pax3^{flag} infection (Fig. 1F). These Pax3-induced structures ultimately began to dissociate 10 to 12 days postinfection, cells eventually reverting to an appearance indistinguishable from uninfected cells (data not shown). Reversion coincided with the loss or significant reductions in the level of Pax3 expression, determined by western analysis. This reversion is consistent with specific levels of Pax3 expression being required to initiate and to maintain the observed morphological changes.

Pax3 induces a Wnt/PCP signaling cascade

The cell rearrangements and many of the cell behaviors induced by Pax3 in Saos-2 cells were reminiscent of morphogenetic cell movements observed during gastrulation and neurulation known as convergent extension (Jacobson, 1981; Keller et al., 1985). During convergent extension, where a tissue narrows along one axis while elongating along a perpendicular axis, both polarized cell protrusive activity as well as cell intercalation occurs (Elul et al., 1997; Shih and Keller, 1992). We observed that ectopic Pax3 expression induced convergence-like behavior in Saos-2 cells with groups of cells converging along a single axis to form columns. This convergence-like behavior was associated with episodic and

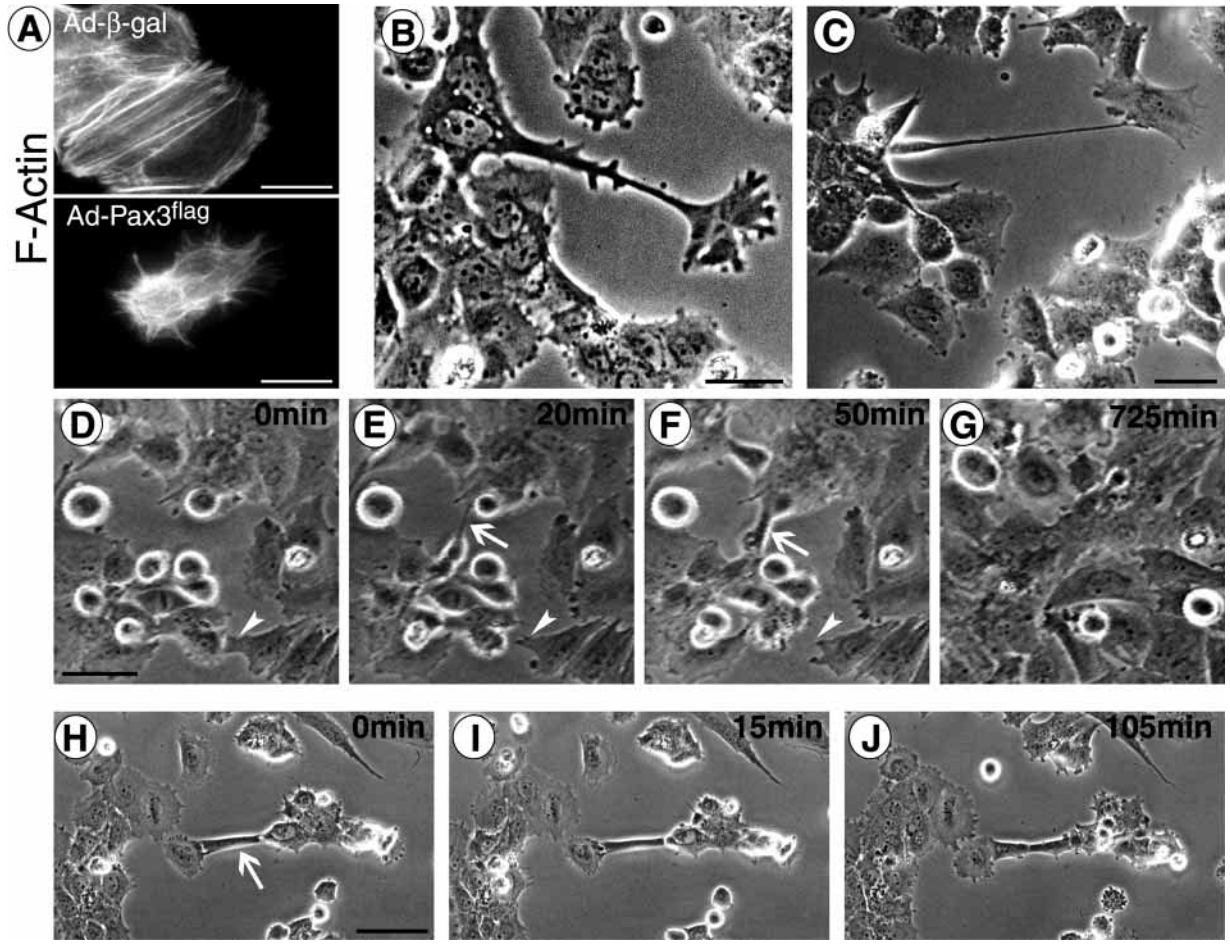

Fig. 4. Ectopic Pax3 expression in Saos-2 cells induces directed cell protrusive behavior. F-Actin staining of Ad-β-gal control infected (A, top panel) or Ad-Pax3^{flag}-infected cells (A, bottom panel) at 72 hours postinfection illustrates the presence of multiple stable lamellipodia and filopodia-like protrusions in Ad-Pax3^{flag}-infected cells. The episodic nature of these protrusions is illustrated by the retraction of a lamelliform protrusion (arrowhead) in sequential stills (D-G) from a time-lapse recording of Pax3-infected cells. Pax3-induced cell protrusions were often elaborate, resembling growth cones (B). Stable filopodia-like protrusions from individual cells were frequently observed to be directed at neighboring cells (C and arrow in E). Time-lapse analysis revealed that these protrusions were involved in cell behavior that resulted in fusion of aggregates (D-G) and in recruitment of free cells to aggregates (H-J) (see text for details). Note cell extending from aggregate to neighboring cell (arrow in H). Bars, 20 μm (A); 40 μm (B,C); 50 μm (D); 80 μm (H).

directed cell protrusive activity, as well as cell intercalative behavior. Given the specific morphological changes of Pax3-expressing Saos-2 cells, we hypothesized that Pax3 may induce activation of a Wnt/PCP-signaling cascade. To test this hypothesis we determined whether factors in the Wnt-signaling pathway known to mediate convergent extension and PCP would behave in a characteristic manner indicative of activation of this signaling cascade. Thus, we first examined whether Dishevelled is recruited to the plasma membrane, as occurs during Frizzled-dependent PCP signaling (Axelrod, 2001; Axelrod et al., 1998).

We examined the subcellular distribution of Dishevelled by indirect immunofluoresence confocal microscopy, using an antibody that recognizes all three known human Dishevelled proteins (Fig. 5). The staining pattern of Dishevelled in both uninfected and Ad-β-gal-infected Saos-2 cells was identical. In both instances, punctate vesicular cytoplasmic staining was observed. The staining pattern in these cells also suggested that Dishevelled was associated with the cytoskeleton, as has been described previously (Torres and Nelson, 2000). Indeed, dual staining of control infected Soas-2 cells with Dishevelled and phalloidin revealed extensive overlap between Dishevelled and F-actin signals, as well as prominent Dishevelled localization along F-actin stress fibers. In contrast to control infected cells, in Ad-Pax3^{flag}-infected cells between 48 to 72 hours postinfection, there was significant accumulation of Dishevelled at the cell cortex, at the tips of filopodia-like protrusions, at cell-cell junctions and peripherally around the nucleus. In Ad-Pax3^{flag}-infected cells, Dishevelled also colocalized with F-actin primarily with actin bundles at the cell cortex and at cell-cell junctions. Distinct from its association with the actin cytoskeleton, Dishevelled did not show any appreciable overlap with microtubules in the presence or absence of Pax3, as determined by dual staining with β-tubulin antibodies (data not shown). Thus, Pax3 induces altered subcellular distribution of Dishevelled, including strong membrane localization, consistent with the potential activation of a Wnt/PCP signaling cascade.

The subcellular distribution of endogenous Frizzleds, which act upstream of Dishevelled in the PCP signaling cascade, has not been previously described in mammalian cells. Using commercially available antibodies to Frizzled 2, which also detect Frizzled 1 due to the high degree of amino acid similarity between Frizzled 1 and Frizzled 2, we examined the subcellular localization of Frizzled in Saos-2 cells (Figs 6, 7). Immunofluorescence confocal microscopy of methanol/acetone-fixed uninfected, Ad-βgal- and Ad-Pax3^{flag}-infected cells revealed strong membrane staining at sites of lamellipodia and filopodia protrusions, strong membrane staining at sites resembling focal adhesions and diffuse punctate cytoplasmic staining (Fig. 6A-C, respectively). Identical staining patterns were observed in paraformaldehyde-fixed cells (Fig. 6D,E), with the exception that an accumulation of vesicular cytoplasmic staining in cells expressing Pax3^{flag} was more apparent. Like that observed for Dishevelled, the staining pattern of Frizzled suggested it was associated with the cytoskeleton. Dual staining of paraformaldehyde-fixed cells with Frizzled and phalloidin revealed that in uninfected and control infected Saos-2 cells, Frizzled colocalizes with F-actin along stress fibers, with a concentration of Frizzled signals at the tips of stress fibers (Fig. 6F-H, strong nuclear Frizzled staining is an artifact of the paraformaldehyde fixation procedure used). In Ad-Pax3^{flag}-infected cells, there is also a dramatic accumulation of Frizzled in cytoplasmic vesicles, corresponding to significant reductions in the number of stress fibers and focal adhesions in these cells (Fig. 6I-K; Fig. 7G-I) (Wiggan et al., 2002). In both control infected and Ad-Pax3^{flag}-infected cells, Frizzled also showed near perfect overlap with F-actin at the leading edge of lamellipodia and at the tips of filopodia (data not shown). Like Dishevelled, there was no appreciable overlap of Frizzled staining with that of microtubules in the presence or absence of Pax3 (data not shown). Thus, these results reveal the localization of both Frizzled and Dishevelled to the actin cytoskeleton.

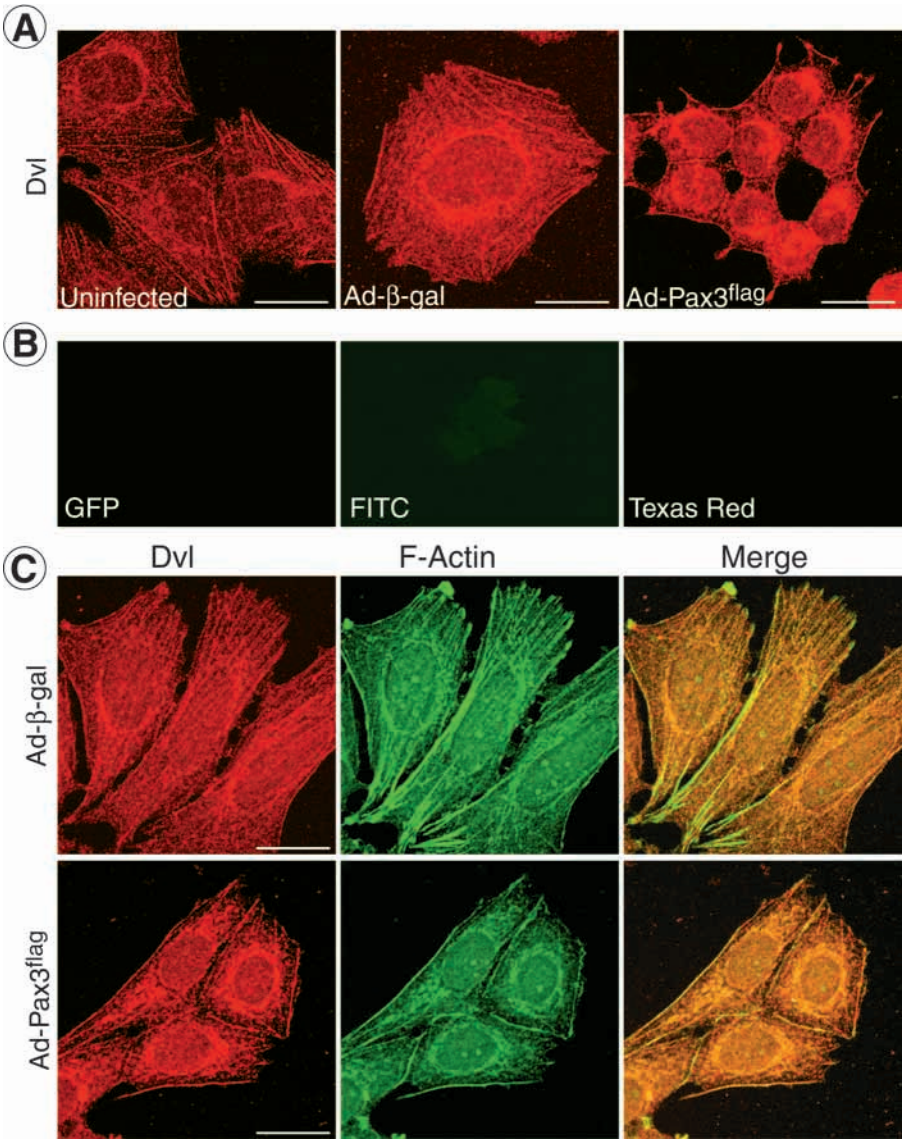

Fig. 5. Subcellular distribution and relocalization of endogenous Dishevelled in Saos-2 cells in response to Pax3 expression. Confocal images of methanol/acetone-fixed Ad-β-gal-infected (A, middle panel) and Ad-Pax3^{flag}-infected (A, right panel and B) cells, at three days postinfection, and uninfected (A, left panel) cells. Methanol/acetone fixation results in complete extraction of virally encoded GFP (B, left panel), with minimal staining with control FITC- (B, middle panel) or Texas Red-conjugated (B, right panel) secondary antibodies. In control cells Dishevelled staining is punctate and cytoplasmic with prominent staining along stress fibers where Dishevelled colocalizes with that of F-actin (C, top row). In cells expressing Pax3, Dishevelled accumulates at the plasma membrane and at cell-cell junctions where it colocalizes with cortical actin bundles (A, right panel; and C, bottom row). In Pax3-expressing cells, Dishvelled also accumulates peripherally around the nucleus and at the tips of filopodia-like protrusions. Bars, 20 μm.

The concentration of Frizzled at the tips of stress fibers predicted a potential association with focal adhesions. We therefore examined whether Frizzled colocalized with the focal adhesion proteins vinculin and paxillin. In uninfected and control Ad-β-gal-infected cells, Frizzled signals overlapped almost perfectly with those of vinculin (Fig. 7) and paxillin (data not shown) at sites of focal adhesions. In Ad-Pax3^{flag}-infected cells there was a significant reduction of Frizzled at focal adhesion sites. Like Frizzled, vinculin also exhibited vesicular cytoplasmic staining in Pax3^{flag}-expressing cells and there was considerable overlap between both proteins at these vesicular structures (Fig. 7G-I). The subcellular distribution of Frizzled and its association with vinculin was pursued further by biochemical fractionation and immunoprecipitation experiments (Fig. 7J,K). Extracts of Saos-2 cells were partitioned into detergent-soluble and -insoluble fractions and

western blots probed with α-Frizzled antibodies (Fig. 7J). Frizzled products were detected almost exclusively in the detergent-insoluble fraction, supporting its association with the actin cytoskeleton. The Frizzled antibodies detected two doublets in insoluble extracts; the upper band of the first doublet migrated at 75 kDa, whereas the upper band of the second doublet migrated at 65 kDa. The 65 kDa band is close to the predicted size of human Frizzled 2 (predicted size 63 kDa), whereas the 75 kDa band is close the predicted size of human Frizzled 1 (predicted size 72 kDa). The lower bands of the two doublets may represent degradation products or, alternatively, they may represent post-translational modified Frizzled products. As Fig. 7K illustrates, both the 75 kDa and 65 kDa Frizzled products co-immunoprecipitated with vinculin from detergent-insoluble extracts (lanes 7 and 8) but not from soluble extracts (lanes 4 and 5), where very little of these proteins localize. Likewise, antibodies directed against Dishevelled, which has recently been shown to associate with other focal adhesion proteins (Torres and Nelson, 2000), co-immunoprecipitated both the 75 and 65 kDa Frizzled products, as well as vinculin from detergent-insoluble extracts (lane 9). Taken together, these results show the association of both Frizzled and Dishevelled to the actin cytoskeleton and complex formation of these proteins with focal adhesion proteins. Our data also reveal that Pax3 expression culminates in the induction of a signaling cascade, which alters the subcellular distribution of both Frizzled and Dishevelled proteins.

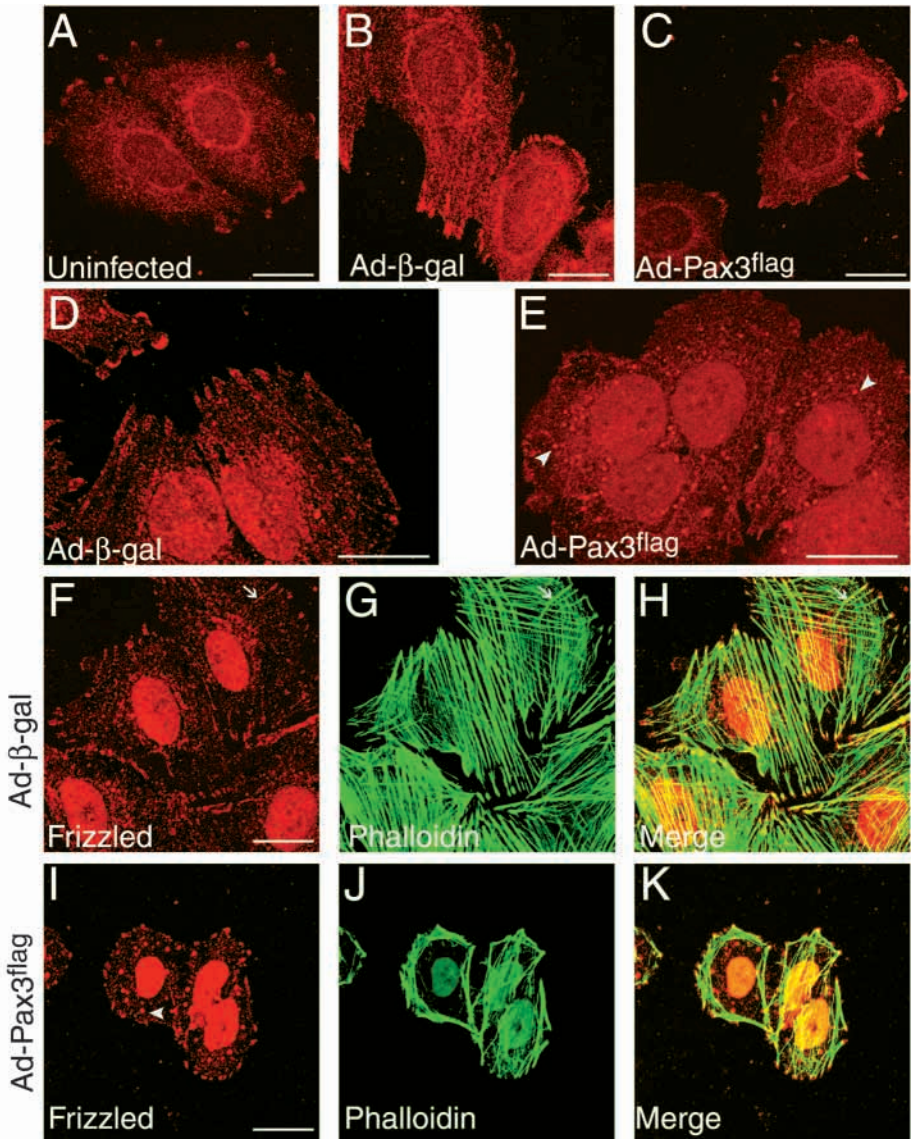

Fig. 6. Localization of endogenous Frizzled to the actin cytoskeleton and its redistribution in Saos-2 cells expressing Pax3. Confocal images of methanol/acetone-fixed (A-C) and paraformaldehyde-fixed (D-K) Saos-2 cells treated as indicated. In control cells (A,B,D) and cells expressing $Pax3^{flag}$ (C,E), Frizzled localized to the tips of protrusions, at sites resembling focal adhesions, and in a punctate diffuse manner throughout the cytoplasm. In control cells Frizzled signals overlapped with those of F-actin (detected by phalloidin staining) along stress fibers (arrow in F-G), with prominent Frizzled signals at the ends of stress fibers (H). Cells expressing $Pax3^{flag}$ have fewer stress fibers (J) relative to control cells (G), and in paraformaldehyde-fixed Pax3-expressing cells, an accumulation of Frizzled signals to cytoplasmic vesicles is apparent (arrowheads in E and I). Cells in F-K were fixed with a paraformaldehyde-cytoskeletal fixation procedure (see Materials and Methods). Bars, 20 μm.

Although PCP signaling in *Drosophila* results in recruitment of Dishevelled to the cell membrane, canonical Wnt signaling has also been reported to induce Dishevelled membrane localization (Boutros et al., 2000). Pax3-induced Dishevelled localization to the plasma membrane did not appear to invoke induction of canonical Wnt signaling, however, as we have shown the absence of changes to the stability and total protein levels of β-catenin (Wiggan et al., 2002). To further examine whether canonical Wnt signaling played a role in Pax3-induced Saos-2 cell aggregation, we generated stable cell lines expressing high levels of either dominant-negative or constitutively active GSK3β (data not shown). Expression of either mutant GSK3β proteins did not inhibit or enhance the kinetics of cell rearrangement or aggregation induced by $Ad\text{-}Pax3^{flag}$ (data not shown). These results further support the notion that Pax3-induced redistribution of Dishevelled and Frizzled in Saos-2 cells does not entail activation of canonical Wnt signaling.

In *Drosophila*, Frizzled- and Dishevelled-mediated PCP signaling results in JNK activation (Boutros et al., 1998). In vertebrates, signaling by Dishevelled also activates JNK (Li et al., 1999; Moriguchi et al., 1999). We therefore determined whether the Pax3-induced recruitment of Dishevelled to the cell membrane and redistribution of Frizzled was associated

with activation of JNK. Using an anti-phospho-JNK-specific antibody, activated JNK was detected at focal adhesions in Ad-β-gal-infected cells (Fig. 8A,C) and in small focal complexes, in Ad-Pax3^{flag}-infected cells (Fig. 8B,D). In these cells, diffuse cytoplasmic and nuclear staining was also observed. An obvious increase in nuclear staining of phospho-JNK compared to Ad-β-gal-infected cells was evident 24 hours after Ad-Pax3^{flag} infection (data not shown). Strikingly, two days postinfection and later, there was an intense juxtanuclear or perinuclear multi-vesicular accumulation of activated JNK in Pax3-expressing cells (Fig. 8B,D). In Saos-2 cells transiently expressing HA-tagged JNK, Pax3 also induced juxtanuclear vesicular accumulation of this exogenously expressed JNK as determined by anti-HA staining (Fig. 8D, inset) The juxtanuclear/perinuclear multi-vesicular staining of activated JNK is characteristic for that of the Golgi (Bershadsky and Futerman, 1994). Our preliminary analyses have revealed that Pax3-induced activated JNK colocalized partially with a number of Golgi markers such as GM130 and β-cop (O.W., unpublished). More extensive colocalization of Pax3-induced juxtanuclear vesicular activated JNK was observed for markers such as GS15 and Rab8 (O.W., unpublished), both factors involved in vesicular traffic. Fig. 8E illustrates further that Pax3 induced increased expression levels of JNK protein. Specifically, by 48 hours postinfection, a 1.5 to 2-fold increase in total JNK protein levels was detected in Ad-Pax3^{flag}-infected cells relative to control cells.

Taken together, Pax3 induces a signaling cascade that results in activation of JNK and in the altered subcellular distribution of Dishevelled, Frizzled and activated JNK. This signaling cascade is associated with changes in cell morphology, increased cell motility and cell rearrangements, as well as altered arrangement of the cytoskeleton and cell adhesion properties. They further support the notion that Pax3 induces a PCP- or Wnt-signaling cascade that gives rise to morphological changes in Saos-2 cells in vitro, analogous to those observed during convergent extension cell movements in vivo.

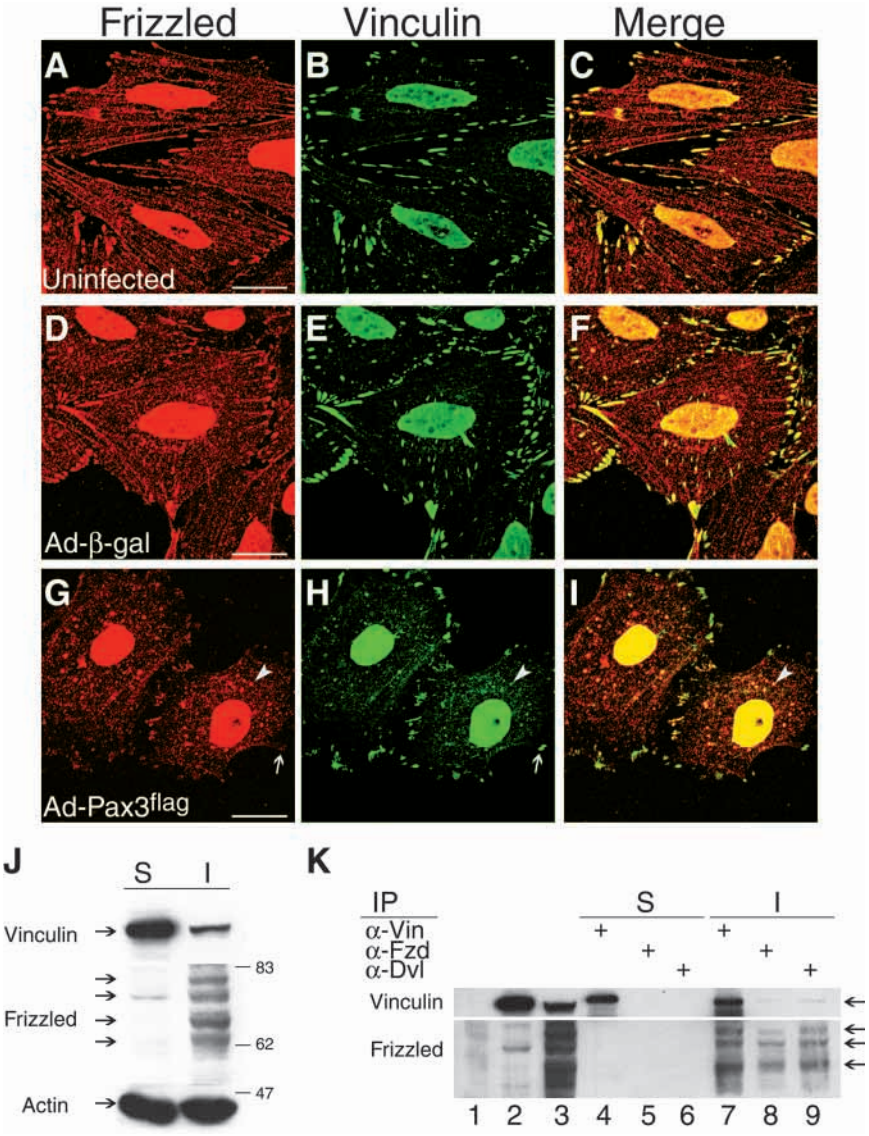

Fig. 7. Frizzled colocalizes with vinculin and co-immunoprecipitates with vinculin from NP-40 detergent-insoluble cell extracts. Uninfected (A-C), Ad-β-gal-infected (D-F) and Ad-Pax3^{flag} infected (G-H) paraformaldehyde (cystoskeletal)-fixed cells were dual labeled with anti-Frizzled (A,D,G) and anti-vinculin (B,E,H) antibodies. Confocal images of dual-stained cells shows near perfect overlap of Frizzled with vinculin at focal adhesions in control cells. In cells expressing Pax3 there was a reduction of Frizzled signals at many vinculin-containing focal adhesions (arrow in G and H); in these cells Frizzled signals overlapped extensively with vinculin in cytoplasmic vesicles (arrowhead in G-I). Strong nuclear staining of Frizzled and vinculin appeared to be an artifact of paraformaldehyde-cytoskeletal fixation. The subcellular distribution of Frizzled was examined by western blots of uninfected Saos-2 cell extracts fractionated into NP-40 soluble (S) and cytoskeletal-associated insoluble (I) extracts (J). (K) Frizzled co-immunoprecipitates with vinculin (lanes 7) and vice versa (lane 8) from insoluble extracts but not from soluble extracts (lanes 4 and 5, respectively) of uninfected Saos-2 cells. Dishevelled antibodies co-immunoprecipitate both vinculin and Frizzled from insoluble extracts (lane 9). Lane 1 represents control immunoprecipitation (IP) of insoluble extracts with IgG. Lane 2 represents 12.5% of input soluble extract and (lane 3) represents 25% of input insoluble extract used for IP. Bars, 20 μm (A,D,G).

Discussion

The cellular and molecular processes regulated by the Pax genes and the mechanisms by which they direct morphogenesis remain largely undefined. Previously we showed that Pax3 induces cell aggregation and a phenotypic mesenchymal-to-epithelial transition in Saos-2 cells. We showed here that Pax3-induced Saos-2 cell aggregation is a result of a number of distinct cell behaviors that are associated with the induction of a conserved non-canonical Wnt-signaling cascade leading to

JNK activation. Our studies have revealed that components of the Wnt/PCP-signaling cascade have distinct subcellular distributions and provide insights to the cellular processes that are regulated by this cascade.

Pax3 induced a distinctive set of cell behaviors during aggregation, where convergence on a single axis resulted in the formation of columns of cells. This convergence is associated with the formation of many persistent lamellipodia and filopodia-like protrusions. Convergence resulted from cell migration, cell intercalation and changes to cell shape and size. These Pax3-induced cell movements are reminiscent of the convergent extension cell movements that occur during *Xenopus* gastrulation and neurulation. Particularly intriguing is the observation that, during neural tube closure in *Xenopus*, the neuroepithelial cells that undergo cell intercalation and convergent extension cell movements express Pax3 (Davidson and Keller, 1999). Pax3-induced convergence behavior in vitro did not appear to be accompanied by significant amounts of extension, as extension appeared to be countered by the dramatic size reduction in Pax3-expressing cells. Our evidence that Pax3 can induce convergence behavior in vitro suggests, however, that Pax3 may regulate convergent extension movements of neuroepithelial cells in vivo. This role for Pax3 is supported further by our data showing that Pax3 induces the same Wnt-signaling cascade in vitro that plays a regulatory role in convergent extension movements in vivo. Although the mechanism by which Pax3 induces this Wnt/PCP-signaling cascade is not yet clear, a compelling possibility is that Pax3 directly or indirectly induces expression of a Wnt or of some other unknown PCP ligand. We are currently determining whether ectopic Pax3 induces expression of endogenous Wnt proteins.

Work by Heisenberg et al. (Heisenberg et al., 2000) showed that Wnt signaling regulates convergent extension movements. In both vertebrate convergent extension movements and polarization of epithelial cells in *Drosophila*, signaling downstream of Frizzled does not elicit the canonical Wnt/Wg signaling cascade (Axelrod et al., 1998; Boutros et al., 1998; Tada and Smith, 2000). Rather, in both instances, signaling by Frizzled results in relocalization of Dishevelled to the plasma membrane (Axelrod, 2001; Axelrod et al., 1998; Wallingford et al., 2000). Mutations to Dishevelled protein that prevent its membrane localization correlate with their ability to block both PCP signaling and convergent extension movements (Axelrod, 2001; Wallingford et al., 2000). Our results show that, in Saos-2 cells, Pax3 induces a Wnt/PCP signaling cascade causing relocalization of Dishevelled to the plasma membrane. The cortical staining pattern of Dishevelled in Pax3-xpressing Saos-2 cells is highly indicative of activation of the PCP branch of the Wnt-signaling cascade. Torres and Nelson (Torres and Nelson, 2000) recently showed that Wnt1 induces actin cytoskeleton reorganization and altered Dishevelled subcellular distribution in embryonic kidney metanephric mesenchymal cells. Interestingly, although Dishevelled associates with the actin cytoskeleton in these cells, Wnt1 stimulation did not cause cortical Dishevelled accumulation, nor was activation of JNK apparent in these cells. Thus, consistent with the work of Axelrod et al. (Axelrod et al. 1998; Axelrod, 2001), it appears that recruitment of Dishevelled to the cell cortex is specific to PCP signaling. Additionally, in Pax3-expressing Saos-2 cells there is no apparent activation of the canonical Wnt-signaling cascade, as evidenced by a lack of altered β-catenin stability or the ability of GSK3β mutants to alter the cellular response to Pax3

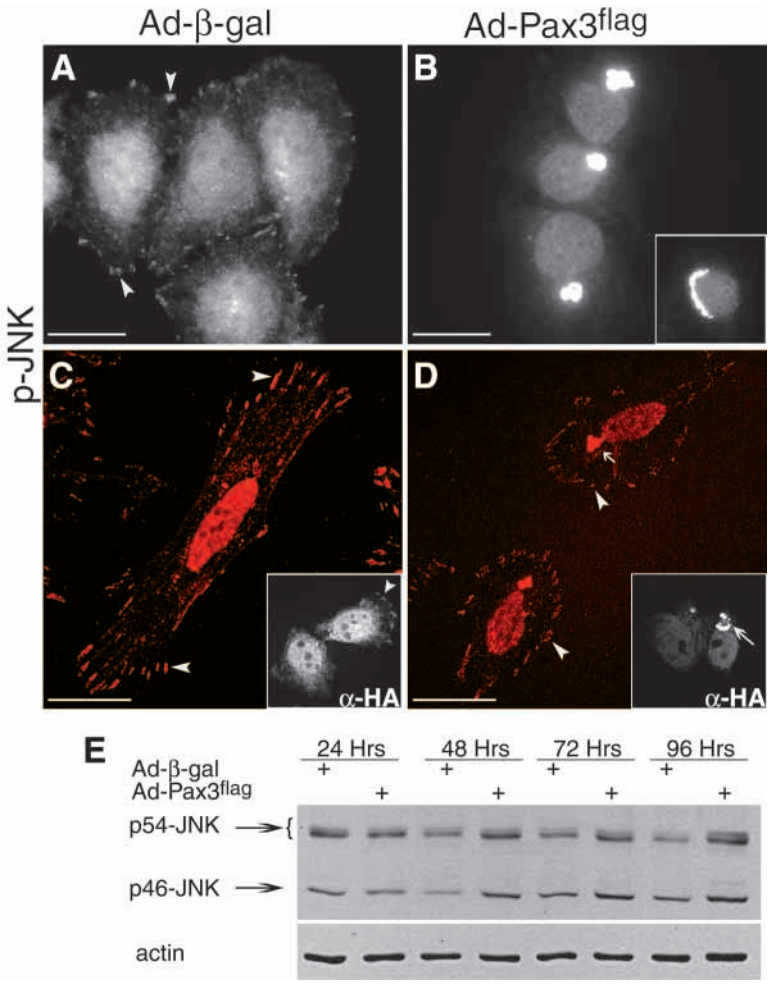

Fig. 8. Ectopic Pax3 induces JNK activation and its accumulation in cytoplasmic multivesicular structures. Saos-2 cells were infected with control (Ad-β-gal) (A,C) or Ad-Pax3^{flag} (B,D) adenoviruses. At three days postinfection cells were fixed with paraformaldehyde (A,B and insets) or paraformaldehyde-cytoskeletal fixation (C,D), and the distribution of (activated) phospho-JNK was determined by indirect fluorescence microscopy. Arrowheads indicate the localization of activated JNK (A,C) and exogenously expressed HA-tagged JNK (C, inset) to focal adhesions in control infected cells. Ad-Pax3^{flag} induces a large increase in activated JNK, which accumulates primarily in juxta-nuclear (B and arrow in D) or perinuclear (B, inset) multivesicular structures as well as at focal complexes (arrowheads in D). Ad-Pax3^{flag} also induces juxtanuclear vesicular accumulation of exogenous HA-tagged JNK (arrow in D, inset). Images in C, D and respective insets are confocal images. Bars, 20 μm. (E) Ectopic Pax3 induces increased JNK expression. Total extracts of control or Ad-Pax3^{flag}-infected Saos-2 cells were harvested postinfection at the indicated times and levels of total JNK proteins assessed by western blotting using an anti-JNK antibody. The same membrane was reprobed for actin as a loading control.

expression. Rather, Dishevelled relocalization is associated with significant activation and relocalization of JNK, further supporting the notion that the Pax3-induced cell behavior in Saos-2 cells relies on signaling cascades similar to those required for convergent extension and PCP morphogenesis.

Our data also indicate that, in Saos-2 cells, Pax3-induced Wnt/PCP signaling may play a role in regulating reorganization of the actin cytoskeleton. In Saos-2 cells, Dishevelled localizes to the actin cytoskeleton with prominent localization along stress fibers. Pax3 induces reorganization of the actin cytoskeleton, causing a reduction in stress fibers and focal adhesions and increased cortical actin bundles, as well as strong actin polymerization at epithelial cell-cell junctions and around the nucleus. In Pax3-expressing cells, Dishevelled colocalized with cortical actin bundles and with actin at cell-cell junctions. Intriguingly, like Dishevelled, Frizzled also localized to the actin cytoskeleton at sites of strong actin polymerization such as at the leading edge of lamellipodia and at the tips of filopodia. Thus, we hypothesize that Pax3-induced Wnt/PCP signaling may regulate the formation and position of actin-rich structures such as lamellipodia and filopodia. Dishevelled regulates the stability and polarization of protrusive activity during *Xenopus* convergent extension movements (Wallingford et al., 2000). Our results indicate that Pax3-induced cell aggregation is associated with increased persistent protrusive activity. Thus, Wnt/PCP signaling may also regulate the turnover of actin structures that give rise to lamelliform and filiform protrusions.

Formation of lamellipodia and filopodia occur in response to Rac and Cdc42, respectively (Kozma et al., 1995; Nobes and Hall, 1995), which are also known mediators of JNK signaling (Coso et al., 1995). The possibility that Rho family GTPases, such as Cdc42 or Rac, may be involved in the JNK signaling cascade induced by Pax3 is intriguing. Genetic analysis in *Drosophila* determined that Rho-family GTPases are upstream mediators of the JNK signaling cascade in dorsal closure, planar tissue polarity and thorax closure (Noselli, 1998; Noselli and Agnes, 1999). It is very likely, therefore, that Rho-family GTPases also participate in the JNK signaling cascade induced by Pax3. Further studies using dominant negative constructs of Rho-family GTPases will be required to address this question. These ongoing studies are expected to define a more precise role for PCP signaling in Pax3-expressing cells.

The localization of Frizzled, Dishevelled and activated JNK to focal adhesions suggests that focal adhesion sites may be primary signaling centers for Wnt/PCP signaling. In Pax3-expressing cells there was a reduction of Frizzled at focal adhesions and an increase in its localization to cytoplasmic vesicular structures. This vesicular accumulation may in part represent internalization of Frizzled due to ligand binding. Pax3-induced Frizzled vesicular accumulation also appears to be associated with a reduction of the cytoskeletal structures with which it associates, such as stress fibers and focal adhesions. Focal adhesion sites represent the major sites of cell-extracellular matrix adhesion in cultured cells. These sites play an important role in cell motility, and large focal adhesions have been reported to retard cell motility (Sastry and Burridge, 2000). Infection by Ad-Pax3^{flag} in Saos-2 cells induced a significant increase in cell motility. Furthermore, cells expressing Pax3 had considerably fewer focal adhesions that were generally smaller in size relative to control infected cells. The localization of Wnt/PCP signaling components to focal adhesions suggests that Wnt/PCP signaling may regulate cell motility, possibly by regulating the dynamics of focal adhesion assembly/disassembly. Indeed, many of the genetically identified signaling cascade components that act downstream of Frizzled and Dishevelled, such as the Rho-family GTPases and Rho-associated kinase, are known regulators of focal adhesion assembly (Sastry and Burridge, 2000; Winter et al., 2001).

PCP signaling results in activation of JNK. Our studies revealed that Pax3 not only induced JNK activation but also induced increased expression levels of JNK protein. Interestingly, the subcellular localization of Pax3-induced activated JNK indicates that the major targets for JNK activity during Wnt/PCP signaling are cytoplasmic rather than nuclear. Specifically, in Saos-2 cells, Pax3-induced activated JNK localizes to a juxtanuclear multivesicular structure. On the basis of preliminary colocalization experiments, this structure appears to be a post-Golgi compartment. In this compartment, activated JNK shows extensive colocalization with Rab8 and GS15. Rab8, a member of the small GTPase family, and GS15, a SNARE protein, are thought have roles in regulating vesicular traffic (Peranen et al., 1996; Xu et al., 1997). Thus juxtanuclear localized activated JNK may play a role in regulating membrane traffic during PCP signaling. This possibility is particularly intriguing given the recent report that a related stress-activated kinase, p38 MAPK, associates with the small GTPase Rab5 to regulate endocytic traffic (Cavalli et al., 2001). The localization of Frizzled, Dishevelled and activated JNK to focal adhesions would suggest further that important Wnt/PCP JNK signaling targets are located at focal adhesion sites.

It has become apparent that signaling cascades involving JNK activation play crucial roles during embryonic morphogenesis in diverse organisms. Genetic analyses in *Drosophila* revealed the importance of the JNK signaling pathway in morphogenetic processes such as dorsal closure, planar cell polarity and thorax closure (Martin-Blanco et al., 2000; Noselli and Agnes, 1999; Zeitlinger and Bohmann, 1999). For these processes, JNK signaling influences cytoskeletal architecture, cell adhesiveness and cell polarity. We speculate that induction of a Wnt/PCP signaling cascade resulting in JNK activation during vertebrate neural tube development may be an important function of Pax3. Like Pax3 mutants, double mutant JNK1 and JNK2 mice also have neural tube closure defects (Kuan et al., 1999; Sabapathy et al., 1999). A role for Dishevelled in neural tube closure in *Xenopus* has also recently been shown (Wallingford and Harland, 2001). We hypothesize that a conserved signaling cascade, involved in the movement and fusion of sheets of epithelial cells in *Drosophila*, has been recruited for vertebrate neural tube closure and that this signaling cascade may be regulated by Pax genes. Analysis of JNK activity in Pax3 mutant mice will be required to determine whether Pax3 influences JNK signaling in vivo.

We thank J. Woodgett and B. Zenke for providing reagents. O.W. wishes to thank Michal Opas, G. A. Candeliere and especially Marc Fadel for extensive help and support throughout this work. Completion of this work would not have been possible without the contributions of these individuals. This work was funded by a grant to P.A.H. from the Canadian Institutes of Health Research.

REFERENCES

Atchley, W. R. and Hall, B. K. (1991). A model for development and evolution of complex morphological structures. *Biol. Rev. Camb. Philos. Soc.* **66**, 101-157.

Axelrod, J. D. (2001). Unipolar membrane association of Dishevelled mediates Frizzled planar cell polarity signaling. *Genes Dev.* **15**, 1182-1187.

Axelrod, J. D., Miller, J. R., Shulman, J. M., Moon, R. T. and Perrimon, N. (1998). Differential recruitment of Dishevelled provides signaling specificity in the planar cell polarity and Wingless signaling pathways. *Genes Dev.* **12**, 2610-2622.

Baldwin, C. T., Hoth, C. F., Amos, J. A., da-Silva, E. O. and Milunsky, A. (1992). An exonic mutation in the HuP2 paired domain gene causes Waardenburg's syndrome. *Nature* **355**, 637-638.

Bershadsky, A. D. and Futerman, A. H. (1994). Disruption of the Golgi apparatus by brefeldin A blocks cell polarization and inhibits directed cell migration. *Proc. Natl. Acad. Sci. USA* **91**, 5686-5689.

Boutros, M., Paricio, N., Strutt, D. I. and Mlodzik, M. (1998). Dishevelled activates JNK and discriminates between JNK pathways in planar polarity and wingless signaling. *Cell* **94**, 109-118.

Boutros, M., Mihaly, J., Bouwmeester, T. and Mlodzik, M. (2000). Signaling specificity by Frizzled receptors in *Drosophila*. *Science* **288**, 1825-1828.

Cavalli, V., Vilbois, F., Corti, M., Marcote, M. J., Tamura, K., Karin, M., Arkinstall, S. and Gruenberg, J. (2001). The stress-induced MAP kinase p38 regulates endocytic trafficking via the GDI:Rab5 complex. *Mol. Cell* **7**, 421-432.

Colas, J. F. and Schoenwolf, G. C. (2001). Towards a cellular and molecular understanding of neurulation. *Dev. Dyn.* **221**, 117-145.

Coso, O. A., Chiariello, M., Yu, J. C., Teramoto, H., Crespo, P., Xu, N., Miki, T. and Gutkind, J. S. (1995). The small GTP-binding proteins Rac1 and Cdc42 regulate the activity of the JNK/SAPK signaling pathway. *Cell* **81**, 1137-1146.

Dahl, E., Koseki, H. and Balling, R. (1997). Pax genes and organogenesis. *Bioessays* **19**, 755-765.

Davidson, L. A. and Keller, R. E. (1999). Neural tube closure in *Xenopus laevis* involves medial migration, directed protrusive activity, cell intercalation and convergent extension. *Development* **126**, 4547-4556.

Elul, T., Koehl, M. A. and Keller, R. (1997). Cellular mechanism underlying neural convergent extension in *Xenopus laevis* embryos. *Dev. Biol.* **191**, 243-258.

Epstein, D. J., Vekemans, M. and Gros, P. (1991). Splotch (Sp2H), a mutation affecting development of the mouse neural tube, shows a deletion within the paired homeodomain of Pax-3. *Cell* **67**, 767-774.

Gumbiner, B. M. (1996). Cell adhesion: the molecular basis of tissue architecture and morphogenesis. *Cell* **84**, 345-357.

Heisenberg, C. P., Tada, M., Rauch, G. J., Saude, L., Concha, M. L., Geisler, R., Stemple, D. L., Smith, J. C. and Wilson, S. W. (2000). Silberblick/Wnt11 mediates convergent extension movements during zebrafish gastrulation. *Nature* **405**, 76-81.

Jacobson, A. G. (1981). Morphogenesis of the neural plate and tube. In *Morphogenesis and Pattern Formation* (ed. T. G. Connelly, L. L. Brinkley and B. M. Carlson), pp. 233-263. New York: Raven Press.

Keller, R. E., Danilchik, M., Gimlich, R. and Shih, J. (1985). Convergent extension by cell intercalation during gastrulation of *Xenopus laevis*. In *Molecular determinants of Animal Form* (ed. G. M. Edelman), pp. 111-141. New York: Alan R. Liss.

Kozma, R., Ahmed, S., Best, A. and Lim, L. (1995). The Ras-related protein Cdc42Hs and bradykinin promote formation of peripheral actin microspikes and filopodia in Swiss 3T3 fibroblasts. *Mol. Cell. Biol.* **15**, 1942-1952.

Kuan, C. Y., Yang, D. D., Samanta Roy, D. R., Davis, R. J., Rakic, P. and Flavell, R. A. (1999). The Jnk1 and Jnk2 protein kinases are required for regional specific apoptosis during early brain development. *Neuron* **22**, 667-676.

Li, L., Yuan, H., Xie, W., Mao, J., Caruso, A. M., McMahon, A., Sussman, D. J. and Wu, D. (1999). Dishevelled proteins lead to two signaling pathways. Regulation of LEF-1 and c-Jun N-terminal kinase in mammalian cells. *J. Biol. Chem.* **274**, 129-134.

Mansouri, A. and Gruss, P. (1998). Pax3 and Pax7 are expressed in commissural neurons and restrict ventral neuronal identity in the spinal cord. *Mech. Dev.* **78**, 171-178.

Martin-Blanco, E., Pastor-Pareja, J. C. and Garcia-Bellido, A. (2000). JNK and decapentaplegic signaling control adhesiveness and cytoskeleton dynamics during thorax closure in Drosophila. *Proc. Natl. Acad. Sci. USA* **97**, 7888-7893.

Moriguchi, T., Kawachi, K., Kamakura, S., Masuyama, N., Yamanaka, H., Matsumoto, K., Kikuchi, A. and Nishida, E. (1999). Distinct domains of mouse dishevelled are responsible for the c-Jun N-terminal kinase/stress-activated protein kinase activation and the axis formation in vertebrates. *J. Biol. Chem.* **274**, 30957-30962.

Nobes, C. D. and Hall, A. (1995). Rho, rac, and cdc42 GTPases regulate the assembly of multimolecular focal complexes associated with actin stress fibers, lamellipodia, and filopodia. *Cell* **81**, 53-62.

Noselli, S. (1998). JNK signaling and morphogenesis in *Drosophila*. *Trends Genet.* **14**, 33-38.

Noselli, S. and Agnes, F. (1999). Roles of the JNK signaling pathway in *Drosophila* morphogenesis. *Curr. Opin. Genet. Dev.* **9**, 466-472.

Peranen, J., Auvinen, P., Virta, H., Wepf, R. and Simons, K. (1996). Rab8 promotes polarized membrane transport through reorganization of actin and microtubules in fibroblasts. *J. Cell Biol.* **135**, 153-167.

Sabapathy, K., Jochum, W., Hochedlinger, K., Chang, L., Karin, M. and Wagner, E. F. (1999). Defective neural tube morphogenesis and altered apoptosis in the absence of both JNK1 and JNK2. *Mech. Dev.* **89**, 115-124.

Sastry, S. K. and Burridge, K. (2000). Focal adhesions: a nexus for intracellular signaling and cytoskeletal dynamics. *Exp. Cell Res.* **261**, 25-36.

Shih, J. and Keller, R. (1992). Cell motility driving mediolateral intercalation in explants of *Xenopus laevis*. *Development* **116**, 901-914.

Sokol, S. (2000). A role for wnts in morpho-genesis and tissue polarity. *Nat. Cell Biol.* **2**, E124-125.

Tada, M. and Smith, J. C. (2000). Xwnt11 is a target of *Xenopus* Brachyury: regulation of gastrulation movements via Dishevelled, but not through the canonical Wnt pathway. *Development* **127**, 2227-2238.

Tassabehji, M., Read, A. P., Newton, V. E., Harris, R., Balling, R., Gruss, P. and Strachan, T. (1992). Waardenburg's syndrome patients have mutations in the human homologue of the Pax-3 paired box gene. *Nature* **355**, 635-636.

Torres, M. A. and Nelson, W. J. (2000). Colocalization and redistribution of dishevelled and actin during Wnt-induced mesenchymal morphogenesis. *J. Cell Biol.* **149**, 1433-1442.

Uusitalo, M., Heikkila, M. and Vainio, S. (1999). Molecular genetic studies of Wnt signaling in the mouse. *Exp. Cell Res.* **253**, 336-348.

Wallingford, J. B. and Harland, R. M. (2001). Xenopus Dishevelled signaling regulates both neural and mesodermal convergent extension: parallel forces elongating the body axis. *Development* **128**, 2581-2592.

Wallingford, J. B., Rowning, B. A., Vogeli, K. M., Rothbacher, U., Fraser, S. E. and Harland, R. M. (2000). Dishevelled controls cell polarity during *Xenopus* gastrulation. *Nature* **405**, 81-85.

Wiggan, O., Fadel, M. P. and Hamel, P. A. (2002). Pax3 induces cell aggregation and regulates phenotypic mesenchymal-epithelial interconversion. *J. Cell Sci.* **115**, 517-529.

Winter, C. G., Wang, B., Ballew, A., Royou, A., Karess, R., Axelrod, J. D. and Luo, L. (2001). Drosophila Rho-associated kinase (Drok) links Frizzled-mediated planar cell polarity signaling to the actin cytoskeleton. *Cell* **105**, 81-91.

Xu, Y., Wong, S. H., Zhang, T., Subramaniam, V. N. and Hong, W. (1997). GS15, a 15-kilodalton Golgi soluble N-ethylmaleimide-sensitive factor attachment protein receptor (SNARE) homologous to rbet1. *J. Biol. Chem.* **272**, 20162-20166.

Zeitlinger, J. and Bohmann, D. (1999). Thorax closure in *Drosophila*: involvement of Fos and the JNK pathway. *Development* **126**, 3947-3956.